ELSEVIER

Journal of Nuclear Materials 279 (2000) 173–180

journal of nuclear materials

www.elsevier.nl/locate/jnucmat

A thermodynamic evaluation of the U–O system from UO_2 to U_3O_8

Yeon Soo Kim

Argonne National Laboratory, Engineering Division, Idaho Falls, ID 83403-2528, USA

Received 15 November 1999; accepted 24 January 2000

Abstract

Thermodynamic constraints and a modified form of Sieverts law were utilized to evaluate the partial thermodynamic functions of the U–O system from UO_2 to U_3O_8 in the temperature range of 500–1800 K. The *p–C–T* relationships for each phase region obtained in the literature were reassessed and new *p–C–T* relationships in regions where data were scarce in the literature were proposed. The results are presented as the oxygen isobars superimposed on the phase diagram to characterize the system.

1. Introduction

The uranium–oxygen system, although one of the most important metal–oxygen systems because of the use of UO_2 as a nuclear fuel, is not fully developed, especially below 1200 K. Many studies of the *p–C–T* relationships on this system have concentrated on regions close to exactly stoichiometric UO_2 [1–10]. In addition, the equilibrium oxygen pressure data in the literature are inconsistent among themselves.

Reviews on the system can be found in [1,11]. The phase diagram with oxygen pressure isobars above 800°C is found in Refs. [4,11–13].

This study investigates comprehensively the partial molar free energies of oxygen in the U–O system from UO_2 to U_3O_8. By using the techniques described in the following section, the best pertinent *p–C–T* relationship for each phase region is proposed among inconsistent data in the literature, and a *p–C–T* relationship is established for the phase where data are not sufficient. As a result, the U–O system is characterized by superimposing the oxygen isobars on the phase diagram, based on the *p–C–T* relationships established in the present work.

2. Analysis method

Analytical methods explained in the following sections have been applied previously in Refs. [14–18] to the Ti–O, Zr–O, Zr–H, U–Zr–O systems.

2.1. Integral constraint

The integral Gibbs energy of formation of the oxide (U_3O_8) formed by the reaction

$$3UO_2 + O_{2(g),1atm} = U_3O_8 \tag{1}$$

is related to the relative partial molar free energies of oxygen ($\Delta\overline{G}(O_2) = RT\ln p_{O_2}$) over the O/U range from 2 to 8/3 by

$$\Delta G_f^0(U_3O_8) = 3\,\Delta G_f^0(UO_{8/3}) = \frac{3RT}{2}\int_2^{8/3} \ln p\,\mathrm{d}C, \tag{2}$$

where R is the gas constant and p, a function of the O/U ratio C and temperature T, is the equilibrium oxygen pressure (in atm) over the oxide. The standard state for the integral Gibbs free energy of formation has been chosen as UO_2 and 1 atm of O_2 is the reference standard state of the relative partial molar Gibbs free energies in Eq. (2). The theoretical background of Eq. (2) can be found in [19,20].

2.2. Enthalpy constraint

Luo and Flanagan [21] showed that the relative partial molar enthalpy of the gas in equilibrium with the two-phase mixture ($\Delta\overline{H}_{2\theta}$) is related to that of either of the neighboring single-phase ($\Delta\overline{H}$) and the intervening phase boundary (C_{pb}) by

0022-3115/00/$ - see front matter
PII: S0022-3115(00)00019-2

$$\Delta\overline{H}_{2\theta} = \Delta\overline{H} + \frac{R}{2}\left[\frac{\partial \ln p}{\partial C}\right]_T \times \frac{dC_{pb}}{d(1/T)}, \quad (3)$$

where R is the gas constant, p the equilibrium partial pressure over the single phase and $dC_{pb}/d(1/T)$ refers to the boundary composition change with temperature. Eq. (3) is generally used for qualitative comparison between $\Delta\overline{H}$ and $\Delta\overline{H}_{2\theta}$. Since $(\partial \ln p/\partial C)_T$ in a single phase region must be positive; whether $|\Delta\overline{H}_{2\theta}|$ is greater or smaller than $|\Delta\overline{H}|$ depends on the sign of $dC_{pb}/d(1/T)$ at the temperature range under consideration. Eq. (3) also suggests that $\Delta\overline{H}_{2\theta} = \Delta\overline{H}$, if C_{pb} is vertical on a temperature-versus-composition phase diagram, i.e., $dC_{pb}/d(1/T) = 0$.

Eq. (3) is very useful in evaluating partial molar enthalpy data measured in the adjacent regions. These interrelationships have been applied successfully to the analysis of the Zr–H [17] and the Zr–O [15] systems.

2.3. Sieverts law

If we assume that Sieverts law behavior is obeyed for oxygen dissolution up to the terminal solubility of UO_2, then the corresponding equilibrium, $1/2\,O_{2(g)} = O_{diss.}$, yields the following mass action law:

$$\frac{C}{\sqrt{p}} = \frac{C_{pb}}{\sqrt{p_{2\theta}}} = k_s, \quad (4)$$

where C_{pb} (which are the phase boundary compositions between $UO_{2+x}/UO_{2+x} + U_4O_{9-y}$ and $UO_{2+x}/UO_{2+x} + U_3O_{8-z}$ shown in Fig. 1) is the terminal solubility of oxygen in the oxide, $p_{2\theta}$ is the equilibrium pressure of the nearby two-phase region, and k_s is the corresponding Sieverts law constant. Eq. (4) is commonly written using the mole fraction in place of the oxygen-to-metal ratio. The distinction has been discussed in Refs. [14–18,22], all of whom argue that the appropriate concentration unit is the gas-to-metal atom-ratio. Eq. (4) provides an interrelationship among C_{pb}, $p_{2\theta}$, and k_s, which are usually measured independently. Eq. (4) can be rewritten as

$$\ln p = \ln p_{2\theta} + 2\ln\left(\frac{C}{C_{pb}}\right). \quad (5)$$

Eq. (5) is useful to obtain equilibrium pressure of a region where that of the adjacent two-phase region is known.

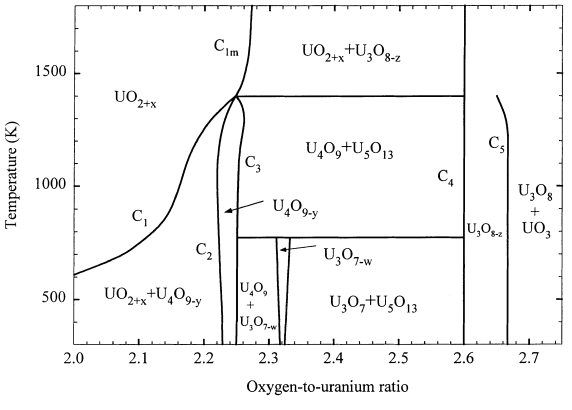

Fig. 1. Phase diagram of the U–O system [11–13].

2.4. Modified form of Sieverts law

Eq. (5) is applicable only to dilute solutions. To account for the systems with extensive gas solubilities, a more generalized form is usually needed in describing gas in equilibrium with its compound, which is expressed by the following p–C–T relationship [14,17,23,24]:

$$\ln p = f(C) + 2\ln g(C) + \frac{h(C)}{RT}. \quad (6)$$

The first- and second-terms on the right-hand side of the above equation result from the thermal and configurational entropy. There are extensive theoretical works in predicting the p–C–T relationship of the M–X systems. Libowitz [23] proposed that $f(C)$ could be a linear function of C but is usually a constant, $h(C)$ is the relative partial enthalpy of gas dissolution, and $g(C) = x/(\xi - C)$ where x is the stoichiometry excess and ξ is usually related to the stoichiometry of the compound.

When applying Eq. (6) to the present case where UO_2 is chosen as the standard state, $x = C - 2$. Hagemark and Broli [2] assumed $\xi = 3$ or 9/4 while Aronson and Belle [3] used $\xi = 3$. For the present work, it is assumed that $\xi = 3$. Eq. (6) reduces to Eq. (5) if $g(C) = C$, and both $f(C)$ and $h(C)$ are constants. However, Lupis [22] and Flanagan and Oates [24] suggested that even if $g(C) = (C-2)/(3-C)$ (with both $f(C)$ and $h(C)$ constants) in Eq. (6), gas solution still follows Sieverts law from the statistical thermodynamics point of view. For the present study, it is also assumed that $h(C) =$ constant and $f(C) = a + bC$ where a and b are constants.

2.5. Applications

In the present analysis, Eqs. (4)–(6) are utilized to establish the p–C–T relationship in regions where data are available but inconsistent. The best p–C–T relationship for each phase region is selected among these available ones. Data are fitted to generate an appropriate relationship where only raw data exist. Eqs. (2) and (3) are used to examine the consistency between the p–C–T relationships established for each phase.

3. Regions in the uranium–oxygen system

Compiling the phase diagram given by Olander [12], which originated from Naito and Kamegashira [11], results in the phase diagram of the U–O system shown in Fig. 1. Roberts and Walter [13] suggested a very similar phase diagram at the low O/U ratio regions.

3.1. UO_{2+x} and $UO_{2+x} + U_4O_{9-y}$

The p–C–T relationship in this region has been studied extensively [1–9]. Lindemer and Besmann [1] proposed the relationship for the UO_{2+x} region:

$$\ln p_{O_2}(UO_{2+x}) = \min(\ln p_1, \ln p_2), \tag{7}$$

where

$$\ln p_1 = 25.7 + 4\ln\frac{2(C-2)(5-2C)}{(9-4C)^2} - \frac{4.33\times10^4}{T}, \tag{7a}$$

$$\ln p_2 = 15.2 + 2\ln\frac{(C-2)(5-2C)^2}{(7-3C)^3} - \frac{3.76\times10^4}{T}, \tag{7b}$$

where p is in atm, C the oxygen to uranium ratio (C = O/U) and T is the temperature in K. Note that C is limited to $C>2$ in Eqs. (7a) and (7b). Aronson and Belle [3] presented an empirical equation based on their experimental result:

$$\ln p_{O_2}(UO_{2+x}) = 4.3 + \frac{31(C-2)}{3-C} - \frac{3.30\times10^4}{T}. \tag{8}$$

Fitting the data of Kiukkola [4] to Eq. (6), the following relationship is obtained (with 99% confidence):

$$\ln p_{O_2}(UO_{2+x}) = -23.0 + 18.2\,C + 2\ln\frac{C-2}{3-C} - \frac{3.62\times10^4}{T}, \tag{9}$$

where $C>2$. Blackburn [6] proposed a model relating oxygen pressure to composition and temperature without using measurement data. He developed his model based on the mass action law considering the equilibrium between the uranium cations and oxygen anions in the solid with oxygen gas. For $C>2$, Blackburn model is given:

$$\ln p_{O_2}(UO_{2+x}) = 10.2 + 2\ln\frac{C(C-2)}{3-C} - \frac{3.29\times10^4}{T}, \tag{10}$$

Naito and Kamegashira [11] presented a $(\log p_{O_2}) - x$ plot based on the data from Refs. [2,4,9] for this region. Similar to Eq. (9), fitting the data obtained from the plot for the UO_{2+x} phase to Eq. (6) yields the following p–C–T relationship:

$$\ln p_{O_2}(UO_{2+x}) = -39.14 + 26.69\,C + 2\ln\frac{C-2}{3-C} - \frac{3.99\times10^4}{T}. \tag{11}$$

where $C>2$. A comparison between the data from Naito and Kamegashira [11] and Eq. (11) is shown in Fig. 2, where Eq. (11) closely fits the data.

Fig. 3 compares Eqs. (7)–(11) at the upper phase boundary as a function of temperature. Eq. (8) lies at the high extreme (i.e., higher oxygen pressure) and Eq. (10) lies at the low extreme for the most temperature region of interest. Eq. (8) does not simulate the asymptotic behavior of UO_2 oxidation at $C = 2.00$ because it does not contain the logarithm term of C. This will eventually yield a large gap at $C = 2.00$ between the UO_{2+x} region and the UO_{2-x} region, which does not follow the nature

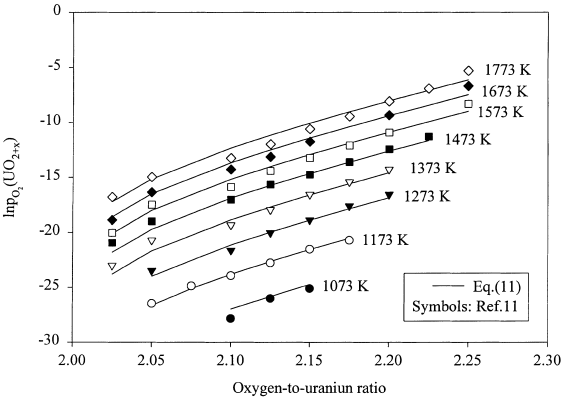

Fig. 2. Comparison between Eq. (11) and the data from Naito and Kamegashira [11] for UO_{2+x} phase.

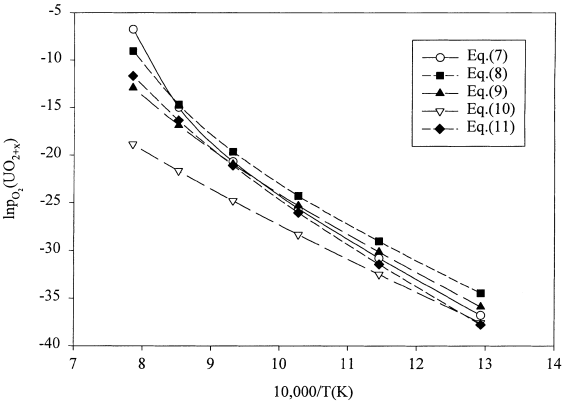

Fig. 3. Comparison of Eqs. (7)–(11).

of the phenomenon. Eqs. (9) and (11) are very close because the Naito and Kamegashira [11] data set originally included those of Kiukkola [4]. Generally, all equations become more consistent at low temperatures. Olander [25] showed that Lindemer and Besmann model (Eq. (7)) and Blackburn model (Eq. (10)) are close at temperatures lower than 1500 K. He used these models for his study because these are the most frequently used ones for studies involving UO_{2+x} [26]. However, Eq. (11) lies between Eqs. (7) and (10) as shown in Fig. 3. Except at high temperatures ($T > 1200$ K), Eq. (11) is closer to Eq. (7) than to Eq. (10). For this reason, Eq. (11) is selected for the UO_{2+x} phase in the present study.

The equilibrium oxygen pressure over the two-phase region $UO_{2+x} + U_4O_{9-y}$ $p_{O_2}(UO_{2+x} + U_4O_{9-y})$ can be found in several places. Lindemer and Besmann [1] provided:

$$\ln p_{O_2}(UO_{2+x} + U_4O_{9-y}) = 22.80 - \frac{4.70 \times 10^4}{T}. \quad (12)$$

Blackburn [5] reported

$$\ln p_{O_2}(UO_{2+x} + U_4O_{9-y}) = 43.57 - \frac{5.9 \times 10^4}{T}. \quad (13)$$

Data obtained from Saito [7] can be expressed as

$$\ln p_{O_2}(UO_{2+x} + U_4O_{9-y}) = 24.46 - \frac{4.86 \times 10^4}{T}. \quad (14)$$

Based on the data measured by Roberts and Walter [13], a similar expression is obtained as

$$\ln p_{O_2}(UO_{2+x} + U_4O_{9-y}) = 45.6 - \frac{7.60 \times 10^4}{T}. \quad (15)$$

Comparing Eqs. (12)–(15), Eqs. (12) and (14) are very close to each other while Eqs. (13) and (15) are inconsistent (see Fig. 4). From this, Eqs. (12) and (14) are considered to be reliable. The enthalpy constraint Eq. (3) requires that $|\Delta\bar{H}_{UO_{2+x}+U_4O_{9-y}}|$ should be larger than $|\Delta\bar{H}_{UO_{2+x}}|$ because $dC_1/d(1/T)$ is negative where C_1 is the phase boundary between UO_{2+x} and $UO_{2+x} + U_4O_{9-y}$. All of the data sets for the two phase region satisfy the enthalpy constraint examined together with Eq. (11). Therefore, the enthalpy constraint alone cannot distinguish which database is better.

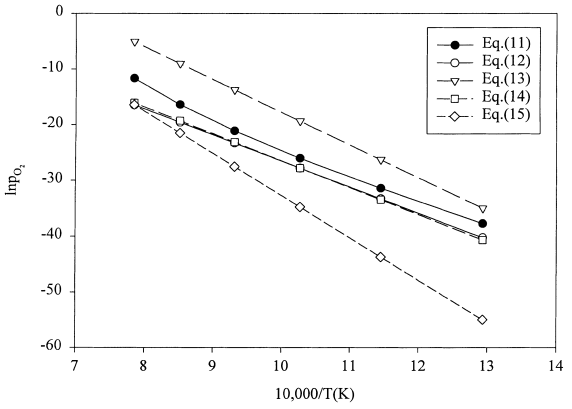

Fig. 4. Consistency evaluation of databases for UO_{2+x} and UO_{2+x}+U_4O_{9-y} regions.

Since the equilibrium pressures at the phase boundary should be continuous, further evaluation of the consistency of Eqs. (12)–(15) with the adjacent phase is possible. Eq. (11) from the UO_{2+x} phase region was extrapolated to the phase boundary between UO_{2+x} and $UO_{2+x} + U_4O_{9-y}$, and compared with Eqs. (12)–(15). From the continuity requirement, the two data sets should match at the phase boundary. The results are shown in Fig. 4. Eqs. (12) and (14) are close to each other and best match Eq. (11). However, Eq. (12) is considered the best because it slightly better match Eq. (11) and provides better result when it is applied in the integral constraint, which is discussed in Section 3.6.

3.2. $UO_{2+x} + U_3O_{8-z}$

Fitting the data for the $UO_{2+x} + U_3O_{8-z}$ phase taken from Ref. [27] yields

$$\ln p_{O_2}(UO_{2+x} + U_3O_{8-z}) = 20.18 - \frac{4.01 \times 10^4}{T}, \quad (16)$$

where p is in atm and T in K. Roberts and Walter [13] presented the following equation for this phase region:

$$\ln p_{O_2}(UO_{2+x} + U_3O_{8-z}) = 18.98 - \frac{3.85 \times 10^4}{T}. \quad (17)$$

Eqs. (16) and (17) are very close to each other. Compared with the extrapolation of $\ln p_{O_2}(UO_{2+x})$ in the UO_{2+x} region to the upper phase boundary, Eqs. (16) and (17) match closely with Eq. (11). This independently confirms that Eq. (11), which also matches well with Eq. (12) in the $UO_{2+x} + U_4O_{9-y}$ region, best represents the UO_{2+x} region. Among Eqs. (16) and (17), Eq. (16) is closer to Eq. (11).

The enthalpy constraint is applied to Eqs. (16) and (17), as was done in Section 3.1. $\Delta\bar{H}$ for the UO_{2+x} region obtained from Eq. (11) is −331.73 kJ/mol. $\Delta\bar{H}$ for $UO_{2+x} + U_3O_{8-z}$ obtained from Eq. (16) is −333.39 kJ/mole and −320.09 kJ/mol from Eq. (17). Since the constraint requires that $|\Delta\bar{H}|$ for $UO_{2+x} + U_3O_{8-z}$ must be larger than that of UO_{2+x}, only Eq. (16) satisfies the constraint. From this result, Eq. (16) is selected for the phase region.

Based on the evaluation in Sections 3.1 and 3.2, it is determined that the best data sets are Eq. (11) for the UO_{2+x} region, Eq. (12) for the $UO_{2+x} + U_4O_{9-y}$ region and Eq. (16) for the $UO_{2+x} + U_3O_{8-z}$ region.

3.3. $U_4O_9 + U_5O_{13}$

Fitting the data picked from Aronson and Belle [3] for this region yields

$$\ln p_{O_2}(U_4O_9 + U_5O_{13}) = 19.39 - \frac{3.94 \times 10^4}{T}. \quad (18)$$

where p is in atm and T in K. Kiukkola [4] presented the expression for this region as

$$\ln p_{O_2}(U_4O_9 + U_5O_{13}) = 18.46 - \frac{3.76 \times 10^4}{T}. \quad (19)$$

Blackburn [5] also provided the following explicit equation:

$$\ln p_{O_2}(U_4O_9 + U_5O_{13}) = 19.40 - \frac{3.94 \times 10^4}{T}. \quad (20)$$

Saito [7] found

$$\ln p_{O_2}(U_4O_9 + U_5O_{13}) = 18.88 - \frac{3.82 \times 10^4}{T}. \quad (21)$$

Roberts and Walter [13] produced

$$\ln p_{O_2}(U_4O_9 + U_5O_{13}) = 20.22 - \frac{4.02 \times 10^4}{T}. \quad (22)$$

All five of the equations for this phase are consistent with one another. For the details, Eqs. (18) and (20) are in good agreement while Eq. (19) is close to Eq. (21). However, the former group lies at the lower extreme and the latter at the upper extreme. Eq. (22) lies between these two extremes. Eq. (22) as well as Eqs. (19) and (21) is rejected because they do not satisfy the enthalpy constraint. Since Eqs. (18) and (20) are basically identical, both data can be selected. However, Eq. (20) is selected to represent this region because it is based on more extensive database. The validity of this determination will be examined later by the enthalpy constraint in Section 3.5 and by the integral constraint in Section 3.6.

3.4. U_4O_{9-y}

The available database for this region was found from Roberts and Walter [13]. However, the data were not sufficient to generate a reliable p–C–T relationship.

A linear interpolation of the data picked at the adjacent phase boundaries is proposed. This method was utilized previously [14]. The data obtained with this method is fitted to Eq. (6), which yields

$$\ln p_{O_2}(U_4O_{9-y}) = -204.9 + 100.8\,C + 2\ln\frac{C-2}{3-C} - \frac{4.0 \times 10^4}{T}. \quad (23)$$

where p is in atm and T in K.

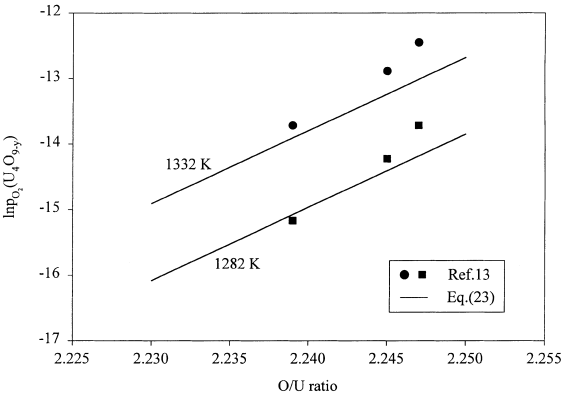

Fig. 5. Comparison between Eq. (23) and the data from Ref. [13] for U_4O_{9-y} phase.

Comparison of Eq. (23) to the experimental data obtained from Roberts and Walter [13] for two temperatures is shown in Fig. 5. Approaching the upper phase boundary, Eq. (23) is lower than the data of Roberts and Walter. However, further comparison of extrapolation of Eq. (23) to the lower phase boundary with the data for the two phase region $UO_{2+x} + U_4O_{9-y}$ shows that this equation is very close to Eq. (12) which best represents the $UO_{2+x} + U_4O_{9-y}$ region. This implies that Eq. (23) is well established.

3.5. U_3O_{8-z}

For this region, data available in the literature are scarce. Fitting the data of Hagemark and Broli [2] obtained for 1373–1573 K and of the values extrapolated from the $UO_{2+x} + U_3O_{8-z}$ phase (Eq. (16)) at the phase boundary C_5 in Fig. 1 yields

$$\ln p_{O_2}(U_3O_{8-z}) = -293.3 + 119.9\,C + 2\ln\frac{C-2}{3-C} - \frac{3.94 \times 10^4}{T}. \quad (24)$$

Since the phase boundary between $U_4O_9 + U_5O_{13}$ and U_3O_{8-z} is vertical, the enthalpy constraint requires that $\Delta\overline{H}_{U_4O_9+U_5O_{13}} = \Delta\overline{H}_{U_3O_{8-z}}$. Applying this requirement to Eqs. (18)–(22), Eqs. (18) and (20) satisfy the requirement. The enthalpy for $U_4O_9 + U_5O_{13}$ obtained from Eqs. (18) and (20) is −327.6 kJ/mol and that of U_3O_{8-z} from Eq. (24) at the phase boundary is also −327.6 kJ/mol. This confirms that the selection of Eq. (20) for $U_4O_9 + U_5O_{13}$ is valid and that Eq. (24) for U_3O_{8-z} has been well established.

3.6. Evaluation of $\Delta G_f^0(U_3O_8)$

Using the integral constraint of Eq. (2), the validity of establishing the p–C–T relationships in previous sections can be examined. The temperature range in which Eq. (2) is applied is confined between 800 and 1500 K. Eq. (2) is interpreted for the temperature range to include the phase regions as follows:

$$\Delta G_f^0(U_3O_8) = \frac{3RT}{2}\left(\int_2^{C_1} \ln p_{O_2}(UO_{2+x})dC' + \int_{C_1}^{C_2} \ln p_{O_2}(UO_{2+x} + U_4O_{9-y})dC' + \int_{C_2}^{C_3} \ln p_{O_2}(U_4O_{9-y})dC' + \int_{C_3}^{C_4} \ln p_{O_2}(U_4O_9 + U_5O_{13})dC' + \int_{C_4}^{C_5} \ln p_{O_2}(U_3O_{8-z})dC'\right), \quad (25)$$

where C_1, C_2, C_3, C_4 and C_5 shown in Fig. 1 are the phase boundaries between UO_2 and U_3O_8.

The molar free energy of formation for the reaction $3UO_2 + O_2 = U_3O_8$ was given as $\Delta G_f^0(U_3O_8) = -342.0 + 0.161T$ (kJ/mol) by Roberts and Walter [13], $\Delta G_f^0(U_3O_8) = -316.8 + 0.142T$ (kJ/mol) by Kubaschewski [19] and $\Delta G_f^0(U_3O_8) = -303.1 + 0.130T$ (kJ/mol) by Barin [28]. The right-hand side of Eq. (25), applying Eqs. (11), (12), (20), (23) and (24), yields $\Delta G_f^0(U_3O_8) = -323.8 + 0.144T$ (kJ/mol). A comparison of $\Delta G_f^0(U_3O_8)$ from Eq. (25) with those from Refs. [13,19,28] is provided in Fig. 6. As is seen in Fig. 6, Eq. (25) generally matches the data from the literature. At temperatures below 1100 K the data from the literature are slightly inconsistent among themselves. In this temperature regime, Eq. (25) is closer to Roberts and Walter [13] and is in accord with all the literature data at higher temperatures. The entropy of Eq. (25), −0.144 kJ/mol K, is closer to that of [19], −0.142 kJ/mol K, than other data.

Overall, the consistency between Eq. (25) and the data in the literature are satisfactory, considering the extensive database used in Eq. (25). This implies that the partial p–C–T relationships used in Eq. (25) to generate the integral property, $\Delta G_f^0(U_3O_8)$, have been well selected. This also implies that these p–C–T relationships best represent their phase regions.

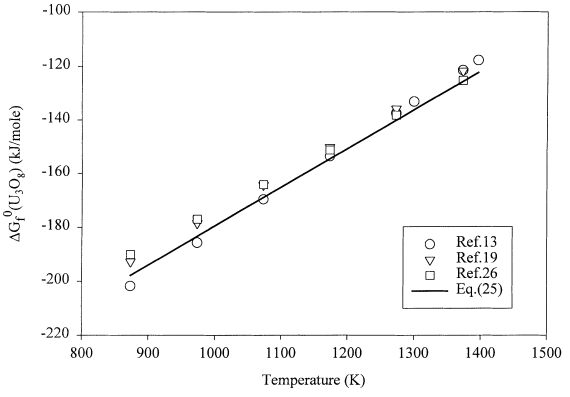

Fig. 6. Comparison of calculated $\Delta G_f^0(U_3O_8)$ from Eq. (25) and the data from the literature.

3.7. Oxygen isobars and the analysis uncertainties

The $p(O_2)$-C–T relationships of oxygen in equilibrium with the uranium oxides from UO_2 to U_3O_8 (Eqs. (11) (12), (16), (20), (23) and (24)) were used to construct the oxygen isobars superimposed on the phase diagram shown in Fig. 7. Above 1300 K, the oxygen isobars agree well with those of Naito and Kamegashira [11]. However, they are approximately two orders of magnitude lower than those of Naito and Kamegashira at temperatures lower than 900 K. However, if the p–C–T relationships that fit Naito and Kamegashira are applied in the integral constraint, $\Delta G_f^0(U_3O_8)$ calculated from Eq. (25) is much higher than all of the experimental data [13,19,28]. This means the Naito and Kamegashira data do not conform with the thermodynamic constraint. Additionally, the validity of the present result is examined with data from other sources [29–31]. The equilibrium oxygen-to-uranium ratios for the given temperature and oxygen pressure from Refs. [29–31] are consistent with the values of the present work.

The good agreement between the isobars of the $UO_{2+x} + U_3O_{8-z}$ region and those of the $U_4O_9 + U_5O_{13}$ region confirms that the partial free energy data for the UO_{2+x}, $UO_{2+x} + U_4O_{9-y}$, and U_4O_{9-y} regions are well established. The isobars of the $UO_{2+x} + U_3O_{8-z}$ region are consistent with those of the UO_{2+x} region, and the isobars of the $U_4O_9 + U_5O_{13}$ region are in agreement

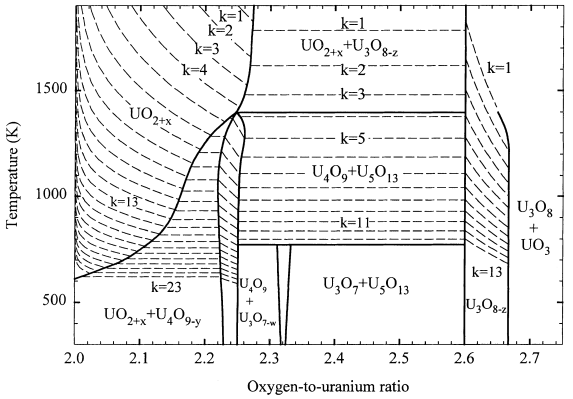

Fig. 7. Revised phase diagram of the U–O system with oxygen pressure isobars superimposed. The isobars are indicated by the index k in $p = 10^{-k}$ where p is in atm.

with those of the UO_{2+x}, $UO_{2+x} + U_4O_{9-y}$ and U_4O_{9-y} regions independently.

Slight mismatches are seen at the phase boundaries C_{1m} and C_4 at temperatures above 1400 K, and discrepancies are also observed at C_1 and C_2 below 800 K. Except for these minor uncertainties, the results obtained overall are satisfactory in general, which demonstrates the consistency between the p–C–T relationships independently obtained. The minor uncertainties seen at the mismatches probably come from two sources. First, although the methodology applied in the approach is based on several valid thermodynamic principles, uncertainties are expected. For instance, the deviation shown in Fig. 7 at low temperatures below 800 K may be due to the Sieverts law assumption (which may not be applicable in this region) or due to the approximations that have larger uncertainties as the temperatures decrease. Second, the uncertainties may be caused by the individually inconsistent database used and the p–C–T relationships generated for the region where available data have been scarce in the literature, particularly for U_4O_{9-y} and $UO_{2+x} + U_3O_{8-z}$ regions. This situation can only be resolved by further experimental investigations.

4. Conclusions

The partial free energy functions of the U–O system have been reviewed using the thermodynamic constraint methods. Consistency among the databases in the UO_{2+x}, $UO_{2+x} + U_4O_{9-y}$, U_4O_9, $U_4O_9 + U_5O_{13}$, $UO_{2+x} + U_3O_{8-z}$ and U_3O_{8-z} phases has been demonstrated. Satisfactory p–C–T relationships have been reassessed using the available experimental data. The p–C–T relationships for U_4O_{9-y} and U_3O_{8-z} regions have been established. The best p–C–T relationships for each phase region to satisfy the thermodynamic constraints and consistency among the databases are

(i) $$UO_{2+x}(C > 2) : \ln p_{O_2}(UO_{2+x}) = -39.14 + 26.69\,C + 2\ln\frac{C-2}{3-C} - \frac{3.99\times 10^4}{T},$$

(ii) $$UO_{2+x} + U_4O_{9-y} : \ln p_{O_2}(UO_{2+x} + U_4O_{9-y}) = 22.80 - \frac{4.70\times 10^4}{T},$$

(iii) $$U_4O_{9-y} : \ln p_{O_2}(U_4O_{9-y}) = -204.9 + 100.8\,C + 2\ln\frac{C-2}{3-C} - \frac{4.0\times 10^4}{T},$$

(iv) $$U_4O_9 + U_5O_{13} : \ln p_{O_2}(U_4O_9 + U_5O_{13}) = 19.4 - \frac{3.94\times 10^4}{T},$$

(v) $$U_3O_{8-z} : \ln p_{O_2}(U_3O_{8-z}) = -293.3 + 119.9\,C + 2\ln\frac{C-2}{3-C} - \frac{3.94\times 10^4}{T},$$

and

(vi) $$UO_{2+x} + U_3O_{8-z} : \ln p_{O_2}(UO_{2+x} + U_3O_{8-z}) = 20.18 - \frac{4.01\times 10^4}{T}.$$

The equilibrium oxygen pressure isobars are shown in the phase diagram (Fig. 7).

Acknowledgements

The author would like to acknowledge Dr D.R. Olander and Dr W. Wang for their suggestions on the analysis method and valuable comments. The author also wish to thank Dr S.L. Hayes of Argonne National Laboratory for his review of the manuscript. This work was supported by the US Department of Energy, Materials/Chemistry, Materials Characterization, under Contract W-31-109-ENG-38.

References

[1] T.B. Lindemer, T.M. Besmann, J. Nucl. Mater. 130 (1985) 473.
[2] K. Hagemark, M. Broli, J. Inorg. Nucl. Chem. 28 (1966) 2837.
[3] S. Aronson, J. Belle, J. Chem. Phys. 29 (1958) 151.
[4] K. Kiukkola, Acta Chem. Scand. 16 (1962) 327.
[5] P.E. Blackburn, J. Phys. Chem. 62 (1958) 897.
[6] P.E. Blackburn, J. Nucl. Mater. 46 (1973) 244.
[7] Y. Saito, J. Nucl. Mater. 51 (1974) 112.
[8] T.L. Markin, R.J. Bones, Atomic Energy Research Establishment, Harwell, England, Harwell Report AERE-R 4042, 1962.
[9] T.L. Markin, R.J. Bones, Atomic Energy Research Establishment, Harwell, England, Harwell Report AERE-R 4178, 1962.
[10] K. Une, M. Oguma, J. Nucl. Mater. 110 (1980) 215.
[11] K. Naito, N. Kamegashira, Adv. Nucl. Sci. Technol. 9 (1976) 99.
[12] D.R. Olander, Nucl. Technol. 74 (1986) 215.
[13] L.E.J. Roberts, A.J. Walter, J. Inorg. Nucl. Chem. 22 (1961) 213.
[14] W. Wang, Yeon Soo Kim, J. Nucl. Mater. 270 (1999) 242.

[15] W. Wang, D.R. Olander, J. Am. Ceram. Soc. 76 (1993) 1242.
[16] D.R. Olander, J. Electrochem. Soc. 131 (1984) 2161.
[17] W. Wang, D.R. Olander, J. Amer. Ceram. Soc. 78 (1995) 3323.
[18] D.R. Olander, W. Wang, J. Nucl. Mater. 223 (1995) 28.
[19] O. Kubaschewski, Metallurgical Thermochemistry, 6th Ed., Pergamon, Oxford, 1992.
[20] M.H. Rand, O. Kubaschewski, The Thermochemical Properties of Uranium Compounds, Oliver and Boyd, Edinburgh, 1963.
[21] W. Luo, T.B. Flanagan, J. Phase Equil. 15 (1994) 20.
[22] C.H.P. Lupis, Chemical Thermodynamics of Materials, Elsevier, New York, 1983, p. 478.
[23] G.G. Libowitz, J. Nucl. Mater. 2 (1960) 1.
[24] T.B. Flanagan, W.A. Oates, B. Bunsenges, Phys. Chem. 76 (1972) 706.
[25] D.R. Olander, J. Nucl. Mater. 270 (1999) 187.
[26] D.R. Olander, private communication, 1999.
[27] Report of The Panel on Thermodynamic and Transport Properties of Uranium Dioxide and Related Phases, IAEA technical reports Ser. No. 39, Vienna, 1965.
[28] I. Barin, Thermochemical Data of Pure Substances, VCH, Weinheim, 1989.
[29] W.V. Lierde, SCK Mol, Belgium, Report D/68/69, 1968.
[30] K. Hagemark, M. Broli, Kjeller, Norway, Report KR-102, 1966.
[31] W. Miekeley, F.W. Felix, J. Nucl. Mater. 42 (1972) 297.